Soil moisture dynamics and response to rainfall under two typical vegetation covers based on HYDRUS-3D

Jing Zhang* and Zhan Liang

The Key Lab of Resource Environment and GIS of Beijing,
Capital Normal University,
#105 West 3rd Ring Road North, Beijing, 100048, China
Email: maggie2008zj@yahoo.com
Email: yqyliangzhan@163.com
*Corresponding author

Abstract: In this study, based on the continuous measurement of soil water content and meteorological parameters, the HYDRUS-3D model was used to simulate the dynamic changes of soil moisture in different soil layers (10–50 cm soil depth) under two typical vegetation covers [alluvial wetland forest (AWF) and ungrazed Bahia grassland (UBG)] in wet and dry seasons in the Alafia River Basin, Florida. Model performance was evaluated using several statistical criteria. Water balance and parameter sensitivity were analysed to indicate the adaptability of the model to the study area. Furthermore, soil moisture variation was assessed under different rainfall levels and its relationships with vegetation type, root biomass and soil physical characteristics were quantitatively and qualitatively analysed. Results showed that the correlation degree between the measured and simulated values of soil water content in the wet and dry periods was higher in the AWF than in the UBG. The water reserves of the UBG were relatively stable. The most sensitive parameters of the model to simulate soil moisture were saturated water content and pore size index. There were significant differences in soil water variation between the two vegetation types. The effect of precipitation on soil moisture was higher under AWF than under UBG.

Keywords: soil moisture dynamic; HYDRUS-3D; precipitation; water balance; sensitivity analysis; soil layer.

Reference to this paper should be made as follows: Zhang, J. and Liang, Z. (2019) 'Soil moisture dynamics and response to rainfall under two typical vegetation covers based on HYDRUS-3D', *Int. J. Water*, Vol. 13, No. 1, pp.26–46.

Biographical notes: Jing Zhang is a Professor of the Capital Normal University in China. Her research interests are in water resources engineering, especially in the areas of integrated hydrological modelling and water quality modelling. Her recent research includes: surface water and groundwater interaction; developing eco-hydrological model in wetland area and exploring new measurement technologies; implementation and applications of remote sensing and GIS in water resources management and modelling.

Zhan Liang graduated from College of Resource Environment and Tourism, Capital Normal University, China. She earned her MS degree in the area of water resources. Her research interests are soil moisture dynamic modelling, and vadose zone modelling.

1 Introduction

Soil water describes moisture present in the soil between the soil surface and the groundwater table (Štekauerová et al., 2006; Asim et al., 2017). Soil water is a major component of the water resource and is the core of conversion and circulation of water (D'Odorico et al., 2010; Legates et al., 2010; Fry et al., 2017). The study of the dynamic characteristics of soil moisture is an indispensable part of the study of the interaction and feedback of terrestrial ecosystems and hydrological processes. Therefore, study of soil water dynamics is of great importance in both agricultural production and ecological hydrology (Seneviratne et al., 2010; Gallego-Elvira et al., 2016).

Previous study of soil water dynamics has largely focused on field observation experiments in undisturbed soil and the numerical simulation and laboratory experiments on disturbed soil (Sandholt et al., 2002; Zhang and Zhang, 2013). Field observation experiments have mainly concentrated on farmland systems. Because of the large number of external factors, the principles of soil moisture movement cannot be fundamentally explained by simple experiments and empirical formulas. Numerical methods are computer-based, have high accuracy and are easily implemented. Therefore, they have become an important means of soil water study (Zhang, 2016). Various types of soil moisture dynamic simulation models are emerging (Slavich et al., 1998; Schlegel et al., 2004; Ranatunga et al., 2008). These models can be divided into system models, conceptual models and mechanistic models (hydrodynamic models). Compared with system models and conceptual models, the Richards equation (based on Darcy's law and continuous equation describing the soil moisture movement and transformation) and the one-dimensional hydrological model are widely used in mechanistic models, but the two-dimensional and three-dimensional applications are less applied (Brunetti et al., 2016).

The HYDRUS-3D model, based on the Richards equation (Šimůnek et al., 2008), is a mature numerical model that can simulate the migration of water, energy and solutes in variably saturated porous media. At present, most research on soil moisture dynamics using the HYDRUS model is based on farmland systems (Kandelous and ŠImůNek, 2010; Al-Ogaidi et al., 2016). In recent years, researchers have made progress in soil moisture research and other related fields. However, studies using the HYDRUS model have mainly focused on farmland systems and laboratory experiments, and arid areas and humid areas have rarely been considered (Satchithanantham et al., 2014). Moreover, few studies have been applied to natural ecosystems, so the HYDRUS model currently has a narrow application range. Soil dynamics, soil migration and the simulation method are important aspects of the study of soil moisture. Therefore, deepening understanding of these aspects is of great importance for the effective use of soil moisture and for vegetation protection.

In this study, the Alafia River Basin in Central West Florida, USA, was selected as the study area. Two typical vegetation types [alluvial wetland forest (AWF) and ungrazed Bahia grassland (UBG)] in this area were studied. The soil moisture under different vegetation was simulated with the HYDRUS-3D model. This paper compares the measured value of field prototype observation system and analogue value, to verify the applicability of HYDRUS-3D in the study area. This paper also considers the effects of vegetation types and rainfall on soil moisture variation. Furthermore, the causes of the change are discussed from the perspective of ecological hydrology. This research enriches the contents and methods of qualitative and quantitative research on soil moisture dynamics in the West Florida region and strengthens the application of HYDRUS-3D model to natural ecosystems. Moreover, this study provides a basis for the further study of vegetation protection and ecological hydrology.

2 Study sites and data collection

The study area was located in Hillsborough County, Florida, close to the Tampa Bay Regional Reservoir in Lithia (Figure 1). Two monitoring wells (USF1 and USF3) are located on the west side of Long Flat Creek and USF1 and USF3 are roughly parallel to Long Flat Creek in the north-south direction. The remaining five monitoring wells (PS39, PS40, PS41, PS42 and PS43) are located from east to west close to Long Flat Creek. The vegetation in the study area transitions from UBG in higher areas (PS43, USF1 and USF3) to AWF (PS43, USF1 and USF3) and the area near the PS42 monitoring well mixes these vegetation types. The rainfall was highly concentrated in June and August (summer humid period) in 2003 and the cumulative rainfall was large. After October (winter drought period), the frequency of rainfall was reduced and the rainfall was relatively small. UBG and AWF are typical vegetation types in Central West Florida. The greatest vegetation coverage occurs in the summer humid period and the lowest density coverage is reached in the winter drought period.

Figure 1 Location of the study area and monitoring wells

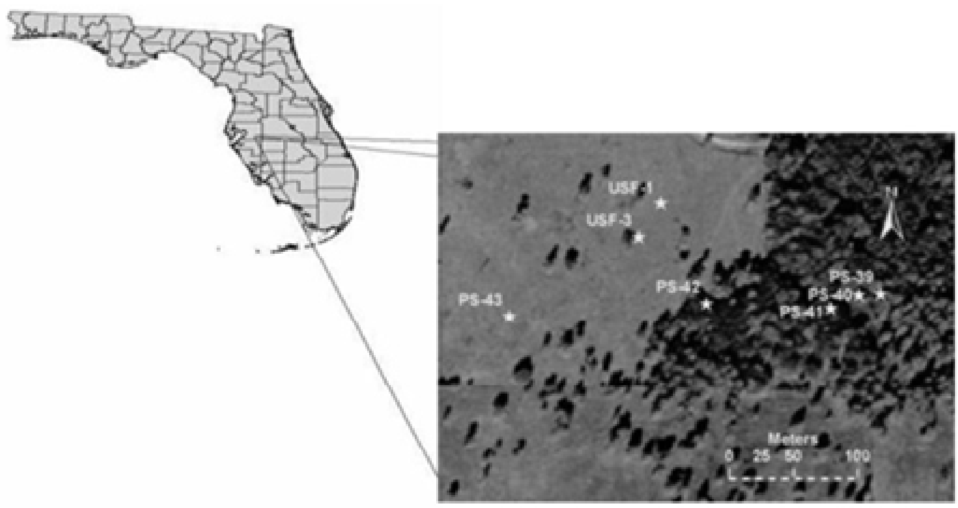

The soil of the study area is mainly Myakka fine sand, the surface layer and the following soil layer have a high permeability (10^{-1} to 10 m/day) according to the soil sample mechanical composition of the PS40 and PS43 wells. The soil samples at several locations on the north-south and east-west cross section show that soils are mainly sandy soil containing clay to about 4 m below the surface of the highlands and about 2.5 m below the surface near the stream. Vertical profiling was conducted with soil moisture probes (EnviroSMART®) installed near the six monitoring wells (PS43, PS42, PS41, PS40, USF1 and USF3), which represent a downhill section from the highland grassland area (PS43) to the riparian forest near the river (USF3). Probes were installed and the hydraulic conductivity of different soil depths in the monitoring wells was obtained. In this study, observations were recorded at 10 min intervals during the observation period (1/1/2002–6/27/2004) and the data were later converted to daily average. Only the top sensor (10 cm) was used to monitor the behaviour of soil moisture content in the vadose zone and the remaining seven sensors monitored the soil moisture content in the low soil moisture content zones. The vegetation near PS40 and PS43 monitoring wells is AWF (including slash pine and hardwood trees) and UBG (Shah, 2007). The hydrological characteristics of the soils at all stations are similar and all the soils are Myakka fine sand (Carlisle et al., 1985).

3 Methodology

3.1 The HYDRUS model

The HYDRUS model was developed by Profs. Kool Huang and Van Genuchten of the National Salty Soil Laboratory, which developed the earliest version of HYDRUS-1D in 1991 and then upgraded to HYDRUS-2D version 2.0 and HYDRUS (2D/3D) version (Provenzano, 2007) in 1999 and 2007, respectively.

The HYDRUS-3D model uses the improved Richards flow control equation (Šimůnek et al., 2006). The numerical solution of the equation is time-discrete using the implicit difference scheme and the spatial distribution of soil profiles is constructed using the Galerkin finite element method. The Richards equation is as shown in equation (1):

$$\frac{\partial \theta}{\partial t} = \frac{\partial}{\partial x}\left[K(\theta)\frac{\partial \varphi_m}{\partial x}\right] + \frac{\partial}{\partial y}\left[K(\theta)\frac{\partial \varphi_m}{\partial y}\right] + \frac{\partial}{\partial z}\left[K(\theta)\left(\frac{\partial \varphi_m}{\partial z} + 1\right)\right] \tag{1}$$

where φ_m is the matrix potential (L), θ is the soil volume water content (L^3/L^3). t is the time (T), x, y and z are the horizontal and vertical coordinates, (L) and $K(\theta)$ is the unsaturated soil conductivity function (L/T) calculated as equation (2):

$$K(h, x, y, z) = K_s(x, y, z)K_r(x, y, z) \tag{2}$$

where K_r is the relative permeability coefficient and K_s is the saturated permeability coefficient (LT^{-1}).

3.2 HYDRUS-3D model setup

In this study, we selected the three-dimensional layered model, the simulation area was assumed to be a cube and the soil layer was set to a three-dimensional symmetrical area of 150 cm × 150 cm × 150 cm, the length of the unit was set to centimetres and the main program selected in the simulation process was the water movement process. The soil moisture was simulated during 2003/6/1–2003/6/30 and 2003/10/5–2003/11/5 at the study area. The time-discrete units were days and the simulation durations were 25 days and 32 days. The initial time step was set to 0.1 days and the minimum and maximum time steps were 0.01 and five days, respectively. The ideal minimum and maximum cycle steps were set as three and seven days, respectively, with a maximum number of cycles of ten and a pressure head tolerance of 1 cm. A total of 968 nodes were set based on the situation of the study area.

The soil water content was the initial condition at the beginning of the simulation. The simulated soil column was divided into nine different soil layers (0, 10, 20, 30, 50, 70, 90, 110 and 150 cm). The data for the 0 cm soil layer was approximately equal to that of the 10 cm soil layer. According to the layout of the field equipment, we took the centre of the soil profile, corresponding the location of instrument monitoring probe, to set the model observation points. An observation point was set for each layer and the observation points were set as far as possible on a vertical line to determine the initial moisture content of the soil.

In the study area, the groundwater level in the wet period is relatively shallow, whereas the groundwater level in the drought period is deep (the average of the groundwater level is below 150 cm). Therefore, the boundary of the wet period (2003/6/1–2003/6/30) was set to deep drainage and the lower boundary of the drought period (2003/10/5–2003/11/5) was set to free drainage. The horizontal effect was ignored in this study and thus the left and right borders were set to impermeable boundaries (Carlisle et al., 1985). Finally, the HYDRUS-3D model was run to produce soil moisture simulations for the two vegetation types. The upper boundary was in direct contact with the atmosphere and was set to the atmospheric boundary. Based on the soil composition of the study area, the soil water characteristic curve parameters were obtained by using the neural network model provided by Rosetta software and the parameters were manually determined according to the measured soil water content (saturated water content, θ_s, the residual moisture content, θ_r, the reciprocal air intake, a, the aperture index, n, the saturated hydraulic conductivity, K_s and the empirical parameter l was 0.5). The soil water characteristic curve parameters for the two vegetation types after calibration are shown in Table 1.

Table 1 Parameters of the soil water characteristic curves of the AWF and the UBG

Vegetation type	*Time*	*Depth (cm)*	θ_r *(cm³/cm³)*	θ_s *(cm³/cm³)*	*a (1/cm)*	*n*	K_s *(cm/day)*
AWF	June	10	0.059	0.345	0.043	1.33	96.09
		20	0.03	0.35	0.063	1.45	60.45
		30	0.05	0.32	0.07	1.71	40.13
		50	0.057	0.34	0.03	1.543	19.272
	October	10	0.081	0.305	0.067	1.586	96.089
		20	0.03	0.315	0.07	1.7	60.48
		30	0.026	0.296	0.073	2.29	50.12
		50	0.035	0.323	0.066	2.11	19.272
UBG	June	10	0.095	0.379	0.015	1.05	0.45
		20	0.125	0.332	0.014	1.14	0.73
		30	0.087	0.286	0.015	1.15	0.38
		50	0.128	0.303	0.015	1.09	0.61
	October	10	0.079	0.372	0.021	1.24	0.27
		20	0.03	0.331	0.035	1.51	0.24
		30	0.03	0.31	0.069	1.78	0.24
		50	0.097	0.295	0.016	1.61	0.36

3.3 Statistics and sensitivity analysis

Five indexes are used in this paper to evaluate the simulation accuracy of the model relative to soil moisture observations under the two kinds of vegetation (Table 2): root mean square error (RMSE), relative error (RE), Nash-Sutcliffe efficiency (NSE) coefficient, correlation (C) coefficient and relative mean absolute error (RMAE).

Table 2 Analysis of soil moisture simulation results of AWF and UBG

Vegetation type	*Well*	*Period*	*Soil layer (cm)*	*RMSE (cm^3/cm^3)*	*RE*	*NSE*	*C*	*RMAE*
AWF (PS40)	PS40	2003/06	10	0.052	0.091	0.621	0.832	0.157
			20	0.056	0.087	0.693	0.857	0.168
			30	0.040	(0.008)	0.886	0.779	0.099
			50	0.030	(0.035)	0.529	0.898	0.184
		2003/10	10	0.012	0.002	0.674	0.864	0.086
			20	0.011	0.007	0.759	0.923	0.100
			30	0.007	(0.023)	0.949	0.988	0.065
			50	0.015	(0.037)	0.990	0.939	0.058
UBG (PS43)	PS43	2003/06	10	0.000	(0.017)	0.589	0.843	0.035
			20	0.014	(0.009)	0.147	0.763	0.046
			30	0.005	(0.008)	0.837	0.938	0.014
			50	0.002	0.006	(0.024)	0.806	0.007
		2003/10	10	0.033	0.046	0.527	0.770	0.093
			20	0.023	0.029	0.757	0.935	0.090
			30	0.020	(0.045)	0.626	0.881	0.070
			50	0.001	(0.001)	(0.155)	0.404	0.003

Note: The numbers in the table with '()' are negative.

In this paper, HYDRUS-3D was used to apply the perturbation analysis method in local analysis to analyse the sensitivity of the parameters. The main parameters of HYDRUS-3D were θ_s, θ_r and K_s and a, n and l are empirical coefficients determining soil unsaturated characteristic curve, where l is usually 0.5. In this paper, the relative change rate of daily soil water content (S_i) caused by parameter and average relative change rate [equation (3)]. The mean sensitivity $\overline{S}$ during the study period was calculated by increasing or decreasing the parameters of θ_s, θ_r, K_s, a and n in a certain soil layer by 10% and 20%, respectively [equation (4)]. The average increase in sensitivity of the parameter by 10% and 20% was taken as the parameter sensitivity (S) [equation (5)].

$$\text{Daily sensitivity } S_i = \frac{Q_i(p \pm \Delta p) - Q_i(p)}{Q_i(p)} \tag{3}$$

$$\text{Mean sensitivity } \overline{S}_m = \frac{\sum_{i=1}^{N} S_i}{N} \tag{4}$$

$$\text{Parameter sensitivity } S = \frac{\sum_{m=1}^{M} \left|\bar{S}_m\right|}{M} \quad (5)$$

where Q_i is the simulated value of soil water content for day i, N is the total number of days for simulation, p is the initial value of the parameter, Δp is the change of input parameter and M is the total number of parameters changed where $M = 4$.

4 Results

4.1 Model applications

In this paper, only the soil moisture between 10 and 50 cm in each monitoring well is simulated and compared. This is because the soil moisture is relatively stable below 50 cm under both vegetation types and rainfall has a great influence on the surface (> 50 cm) soil moisture dynamics. The soil moisture simulations by HYDRUS-3D of the AWF (PS43) and UBG (PS40) in June and October 2003 in the study area are shown in Figures 2–5 alongside the measured values. As shown in Figures 2–5, the simulation of soil moisture of the model on AWF was better than that for UBG. Detailed statistics of the accuracy of the model relative to the observations are shown in Table 3.

Table 3 Water balance analysis of AWF and UBG

Vegetation	*Period*	*Cumulative rainfall (cm)*	*Cumulative transpiration (cm)*	*Cumulative deep seepage(cm)*	*Cumulative soil moisture change (cm)*
AWF	2003/06/06–2003/06/30	19.27	6.40	–0.51	13.38
	2003/10/05–2003/11/05	0.54	8.33	0.13	–7.92
UBG	2003/06/06–2003/06/30	19.27	3.00	16.23	0.04
	2003/10/05–2003/11/05	0.54	2.41	–1.70	–0.06

4.2 Model performance evaluations

Table 3 shows the range of measurement and simulation of soil moisture evaluation parameters RMSE, RE, NSE, C and RMAE in the 10–50 cm soil of the AWF and UBG in June 2003.

The numerical range of the evaluation parameters shows that the simulation accuracy of HYDRUS-3D for AWF was higher than that for UBG in the corresponding time period whether in June or October 2003. At the same time, the simulation accuracy of HYDRUS-3D for AWF in June 2003 (humid period) was significantly lower than that for UBG in October (drought period). The simulation accuracy of HYDRUS-3D for UBG in the 10–50 cm soil in June 2003 was obviously lower than that in October. The NSE of UBG in the 50 cm soil was negative, indicating that the simulation is invalid. Therefore, the suitability of HYDRUS-3D model to this study area requires further verification.

In the process of simulating soil moisture, HYDRUS-3D neglects the effect of surface runoff and the surface runoff coefficient of forested land is less than that of non-forested land. In June 2003, the rainfall was heavy and AWF canopy intercepted a considerable amount of rainfall, which effectively reduced the surface runoff. The surface runoff of the Bahia grassland was large, so the simulation accuracy of HYDRUS-3D for AWF was higher than that for UBG.

Figure 2 Measured and simulated values of soil moisture at four soil depths, (a) 10 cm (b) 20 cm (c) 30 cm (d) 50 cm in AWF (PS40) in June 2003 (see online version for colours)

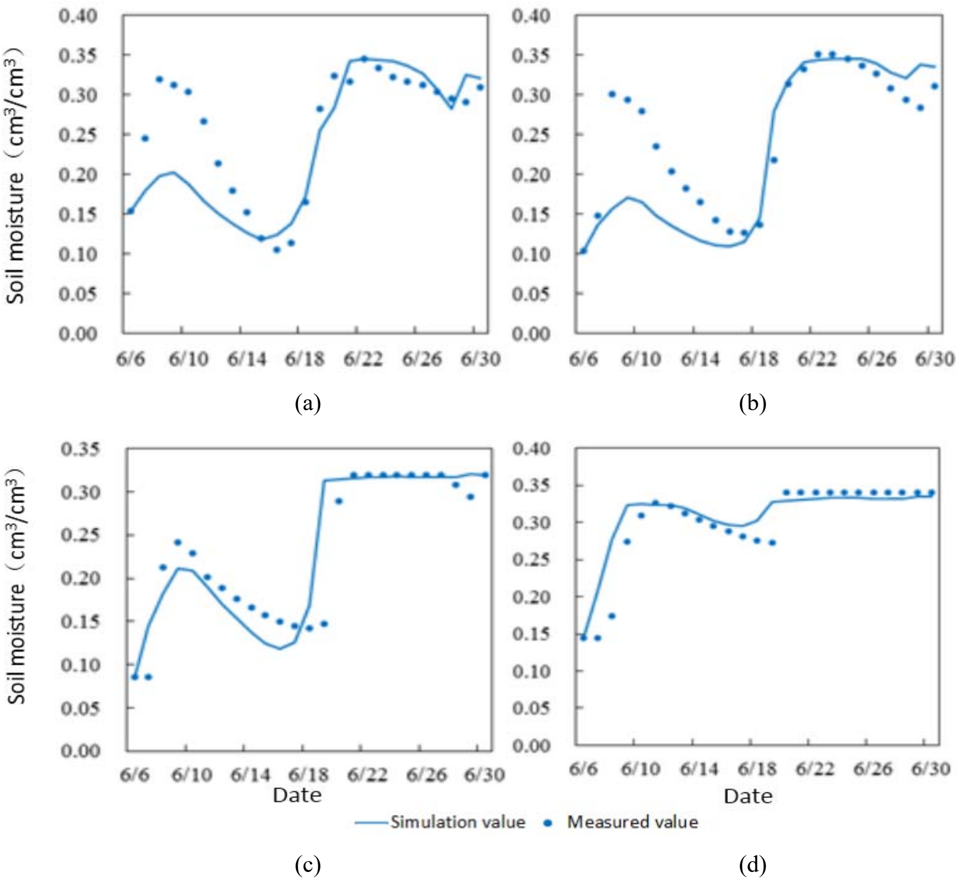

The runoff coefficient increased with the increase of rainfall, whether it is forest land or grassland. When the rainfall was less than 30 mm, the surface soil layers generally did not produce meaningful runoff and the runoff coefficient was very small (< 5%). There was no runoff at all in some forest areas and the runoff coefficient is 0. Therefore, the simulation accuracy in 2003, October was higher than that in June in both AWF and UBG. This was because of the limited rainfall in October, leading to little surface runoff and thus higher simulation accuracy than that of rainy months.

Figure 3 Measured and simulated values of soil moisture at four soil depths, (a) 10 cm (b) 20 cm (c) 30 cm (d) 50 cm in AWF (PS40) in October 2003 (see online version for colours)

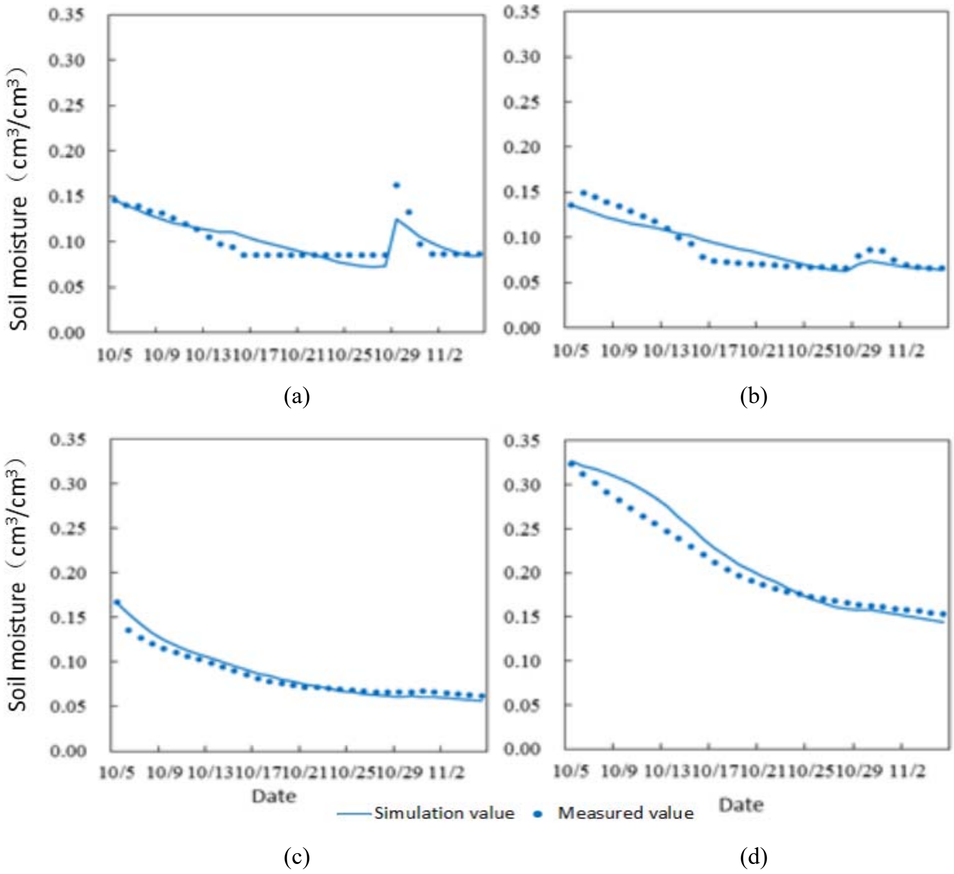

Figure 4 Measured and simulated values of soil moisture at four soil depths, (a) 10 cm (b) 20 cm (c) 30 cm (d) 50 cm in UBG (PS43) in June 2003 (see online version for colours)

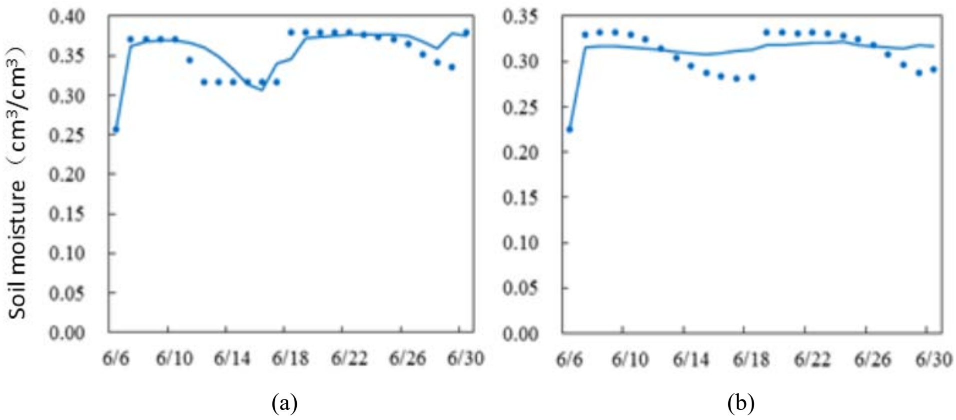

Figure 4 Measured and simulated values of soil moisture at four soil depths, (a) 10 cm (b) 20 cm (c) 30 cm (d) 50 cm in UBG (PS43) in June 2003 (continued) (see online version for colours)

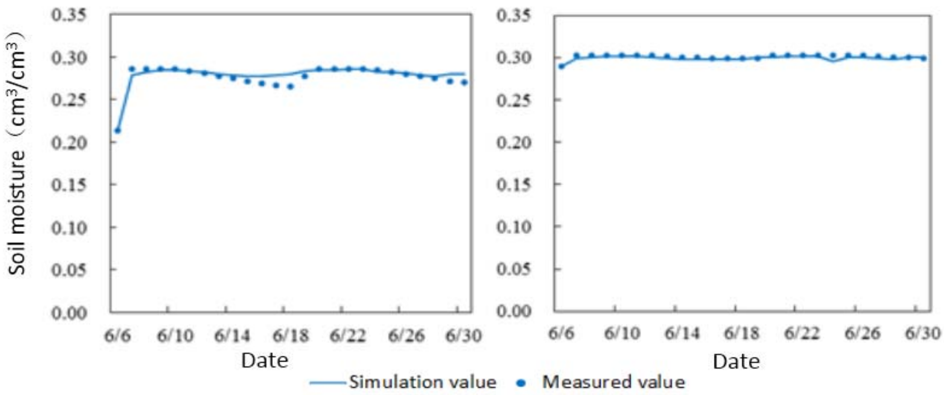

(c) (d)

Figure 5 Measured and simulated values of soil moisture at four soil depths, (a) 10 cm (b) 20 cm (c) 30 cm (d) 50 cm in UBG (PS43) in October 2003 (see online version for colours)

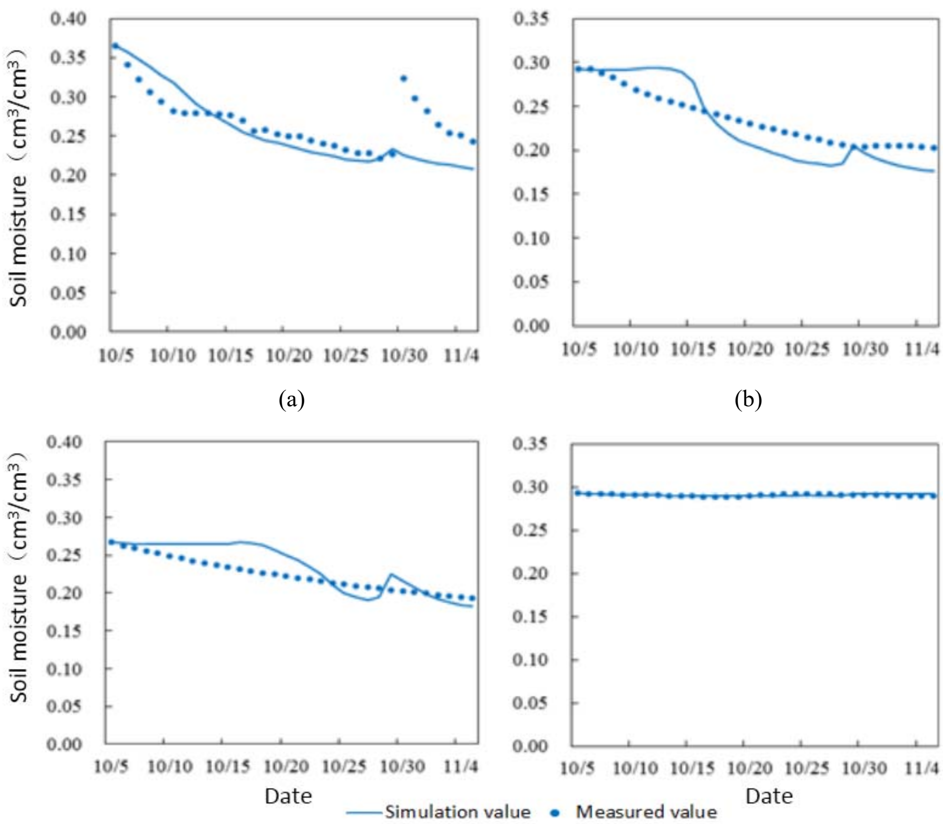

(c) (d)

4.3 Water balance

The water balance of AWF and UBG in the two periods is next analysed according to the water balance equation.

Evapotranspiration is the main loss pathway of soil moisture in the study period. The evapotranspiration of AWF in June 2003 accounted for 33.21% of rainfall and the evapotranspiration in October 2003 was 15.43 times that of rainfall. The evapotranspiration of UBG in June 2003 accounted for 15.57% of rainfall and the evapotranspiration in October was 4.46 times that of rainfall. In both drought periods and humid periods, the evapotranspiration of AWFs was significantly higher than that of UBG. In addition, deep percolation is also an important pathway of soil moisture loss, for example, the amount of deep percolation in soil of UBG in June 2003 was 16.23 cm, which accounted for 84.22% of the rainfall.

In this study, the processes of surface runoff and vegetation interception were ignored and soil was taken to have a direct effect with rainfall in the atmosphere and evapotranspiration. As shown above, infiltration occurs when rainfall is greater than evapotranspiration.

The water balance equation can be expressed as

$$P + G_i + S_i = \mathrm{ET} + S_o + G_o + \Delta W \tag{6}$$

where P is rainfall, G_i and G_o are groundwater recharge and output, respectively, S_i and S_o are surface water recharge and output, respectively, ET is evapotranspiration and ΔW is the change of soil water storage. Combined with the actual situation of this paper, the water balance equation can be simplified as equation (7)

$$P = \mathrm{ET} + D_r + \Delta W \tag{7}$$

where D_r is the soil deep percolation amount. The water balance analysis of AWF and UBG in the two periods is shown in Table 3.

As shown in Table 3, rainfall was relatively high during the humid period of June 2003 and the soil water storage increased in both AWF and UBG; however, the increase of the AWF was much greater than that of the UBG. This was because the soil moisture in the UBG was in a near-saturated state during the humid period; the soil absorbed less rainfall and the moisture infiltrated into the soil mainly leaked through the lower boundary. The increase of water storage in the soil of AWF was not only from rainfall but also from groundwater recharge, mainly because of the shallow groundwater level (150 cm or more) in the humid period. The soil water storage under both vegetation types decreased in drought period of October 2003, but the reduction was largest in the AWF.

This was because the evapotranspiration was much larger than the rainfall in drought period and the evapotranspiration of AWF was 2.78 times that of UBG. The groundwater level of AWF was deeper (below 150 cm) and the soil water was not supplied from the groundwater. The UBG had four days of groundwater level below 150 cm, enhancing the loss of soil water and soil water storage reduction was small.

4.4 Sensitivity analysis

In this paper, the sensitivity of soil moisture characteristic curve parameters calculated by perturbation analysis is shown in Tables 4 and 5 for the wet and dry season, respectively.

Table 4 Soil moisture characteristic curve parameter sensitivity of AWF and UBG in the wet period

Vegetation	*Soil layer*	θ_r	θ_s	*a*	*n*	K_s
AWF (PS40)	10 cm	0.0122	0.0795	0.0117	0.0781	0.0002
	20 cm	0.0069	0.0674	0.0155	0.0870	0.0045
	30 cm	0.0095	0.0597	0.0095	0.0508	0.0030
	50 cm	0.0014	0.0773	0.0060	0.0081	0.0024
UBG (PS43)	10 cm	0.0003	0.0983	0.0044	0.0457	0.0005
	20 cm	0.0025	0.0920	0.0170	0.0410	0.0029
	30 cm	0.0008	0.0876	0.0119	0.0264	0.0003
	50 cm	0.0009	0.0855	0.0008	0.0142	0.0017

Table 5 Soil moisture characteristic curve parameter sensitivity of AWF and UBG in the dry period

Vegetation	*Soil layer*	θ_r	θ_s	*a*	*n*	K_s
AWF (PS40)	10 cm	0.0484	0.0395	0.0087	0.1490	0.0032
	20 cm	0.0010	0.0722	0.0010	0.1611	0.0061
	30 cm	0.0189	0.0668	0.0033	0.1021	0.0051
	50 cm	0.0036	0.0749	0.0235	0.0263	0.0030
UBG (PS43)	10 cm	0.0028	0.0638	0.0047	0.0388	0.0011
	20 cm	0.0014	0.0623	0.0085	0.0282	0.0022
	30 cm	0.0009	0.0256	0.0090	0.0189	0.0002
	50 cm	0.0002	0.0675	0.0008	0.0170	0.0006

These findings indicate that θ_s and *n* parameters of the two soil water characteristic curves were more sensitive; the change of values of these two parameters had a great influence on the output of the model. Moreover, the sensitivity of *n* in AWF was higher than that of UBG, but the value of *n* in the 50 cm soil layer of UBG was less than 0.025, which is moderately sensitive and this difference may be caused by the low simulation accuracy of the model for UBG.

5 Discussions

5.1 Characteristics of soil moisture under typical vegetation

Soil moisture varies both under different types of vegetation within a single research period and under the same type of vegetation but different research periods. This study considered the soil moisture under different vegetation types. Figures 6 and 7 show the change of soil moisture in the AWF and UBG in June and October 2003 monitored by the EnviroSMART soil moisture monitor (measured data only).

As shown in Figure 6 and Table 6 in June 2003 (the wet period), the maximum soil water content of AWF occurred in 10 cm soil layer and the minimum appears at 30 cm. In UBG, the maximum value also occurred at 10 cm soil depth and the minimum value appears in the 30 cm soil layer, both higher than the AWF. At the same time, the average soil water content of the 10–30 cm soil layer was significantly higher than that of AWF and the 50 cm soil layer was lower.

Figure 6 Dynamic change of soil moisture in (a) AWF (PS43) and (b) UBG (PS40) in June 2003 (see online version for colours)

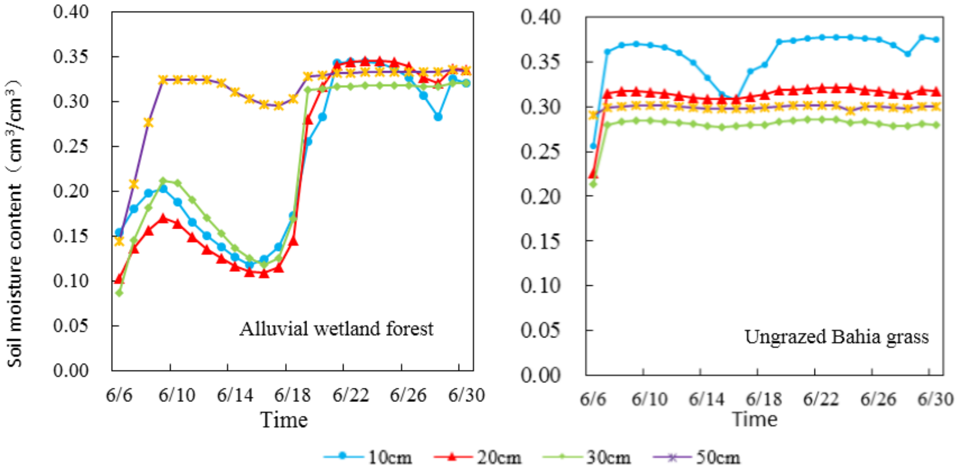

(a) (b)

Figure 7 Dynamic change of soil moisture in (a) AWF (PS43) and (b) UBG (PS40) in October 2003 (see online version for colours)

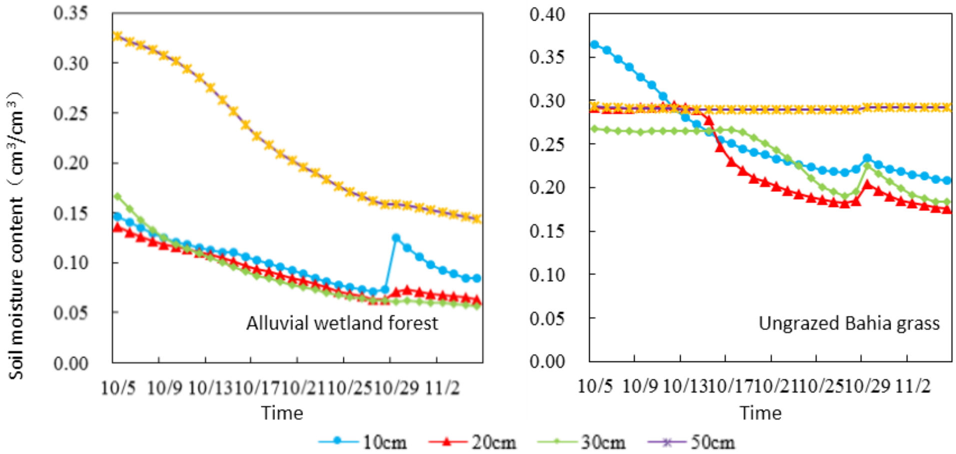

(a) (b)

As shown in Figure 6 and Table 6 in October 2003, the maximum soil water content in the AWF was in the 50 cm soil layer and the minimum was in the 30 cm soil layer. The maximum value was shown in the 10 cm soil layer. The minimum occurred in the 20 cm soil layer. The average AWF of 10–50 cm soil was higher than that of AWF.

Figures 6 and 7 indicate that the soil water content of 10–30 cm soil layer decreased with the increase of soil depth in June and October 2003 and the soil water content increased in the depth range of 30–50 cm. The soil water content of the 10–30 cm soil layer decreased with the increase of soil depth in June 2003 and the soil water content increased from 30–50 cm to 10–20 cm soil depth. Water content showed a downward trend, with increases within the 20–50 cm depth range.

Table 6 Maximum and minimum and average soil moisture content of AWF (PS43) and UBG (PS40) in June and October 2003

Vegetation type	*Period*	*Soil layer*	*10 cm*	*20 cm*	*30 cm*	*50 cm*
AWF	2003/06	Max.	0.3442	0.3450	0.3208	0.3353
		Min.	0.1179	0.1031	0.0862	0.1440
		Average	0.2345	0.2284	0.2330	0.3095
	2003/10	Max.	0.1461	0.1360	0.1668	0.3265
		Min.	0.0717	0.0629	0.0569	0.1444
		Average	0.1025	0.0893	0.0876	0.2177
UBG	2003/06	Max.	0.3774	0.3215	0.2858	0.3018
		Min.	0.2562	0.2249	0.2138	0.2901
		Average	0.3569	0.3120	0.2788	0.2993
	2003/10	Max.	0.3646	0.2943	0.2671	0.2931
		Min.	0.2085	0.1764	0.1831	0.2892
		Average	0.2572	0.2288	0.2346	0.2907

Note: Units: cm^3/cm^3.

5.2 Stability analysis of soil moisture under typical vegetation types

The stability of soil water may be described as the sensitivity of soil water content to environmental changes. In this paper, the coefficient of variation (*Cv*) of soil water content is applied to describe the stability of soil water. According to the size of *Cv*, the soil layers were divided into stable layer ($Cv \le 0.1$), secondary active layer ($0.1 < Cv \le 0.2$), active layer ($0.2 < Cv \le 0.3$) and fast variable layer ($Cv > 0.3$). The standard deviation (*SD*) and *Cv* were calculated as equations (8) and (9):

$$SD = \sqrt{\frac{\sum_{i=1}^{N} (Q_i - Q_{iave})^2}{N}} \tag{8}$$

$$Cv = \frac{SD}{Q_{iave}} \tag{9}$$

where Q_i is the measured value of soil water content in day *i*, Q_{iave} is the mean of the measured values and *N* is the number of days observed.

Table 6 shows that in the June 2003 wet period, the AWF 10–30 cm soil layer *Cv* was within the variable layer category, whereas the 50 cm soil layer was in the secondary active layer category. However, in the UBG in June 2003, the 10–50 cm *Cv* values were within the stable layer category. In October 2003, the *Cv* of 10 cm, 20 cm and 50 cm soil layers in the dry period were within the active layer category. The 30 cm soil layer was in the fast variable layer category, the grazing grass is 10 cm and the 30 cm soil layer was within the secondary active layer category, 20 cm soil layer was in the active layer category and the 50 cm soil layer was in the stable layer category.

For all the circumstances considered in this study (wet period or dry period, the AWF or UBG), the *Cv* of soil water content in the surface soil (10–20 cm) was higher than the soil layer below and the change of soil water content was relatively high. The *Cv* of soil water content was higher than that of grazing grass under the two study periods. We can conclude that the grazing capacity of the UBG is very strong and it has good water conservation ability.

5.3 Soil moisture response to rainfall under typical vegetation

The impact of rainfall on the structure and function of ecosystems is mainly associated with changes to soil moisture. In general, after rainfall (not considering the hysteresis effect), soil moisture will increase rapidly and then gradually decrease because of vegetation transpiration and soil surface evaporation until rainfall occurs again.

Figure 8 Response of soil moisture under AWF and UBG to rainfall at different soil depth, (a) 10 cm (b) 20 cm (c) 30 cm (d) 50 cm in June 2003 (see online version for colours)

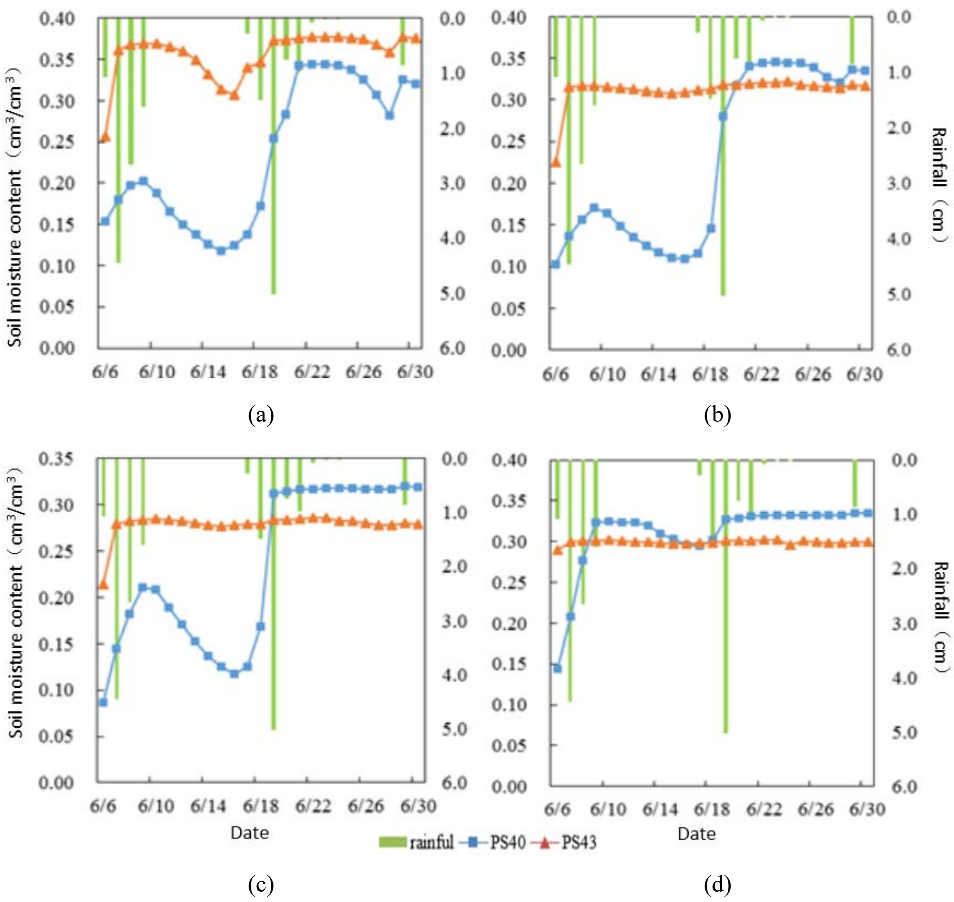

Note: Humid period.

Figure 9 Response of soil moisture under AWF and UBG to rainfall at different soil depth, (a) 10 cm (b) 20 cm (c) 30 cm (d) 50 cm in October 2003 (see online version for colours)

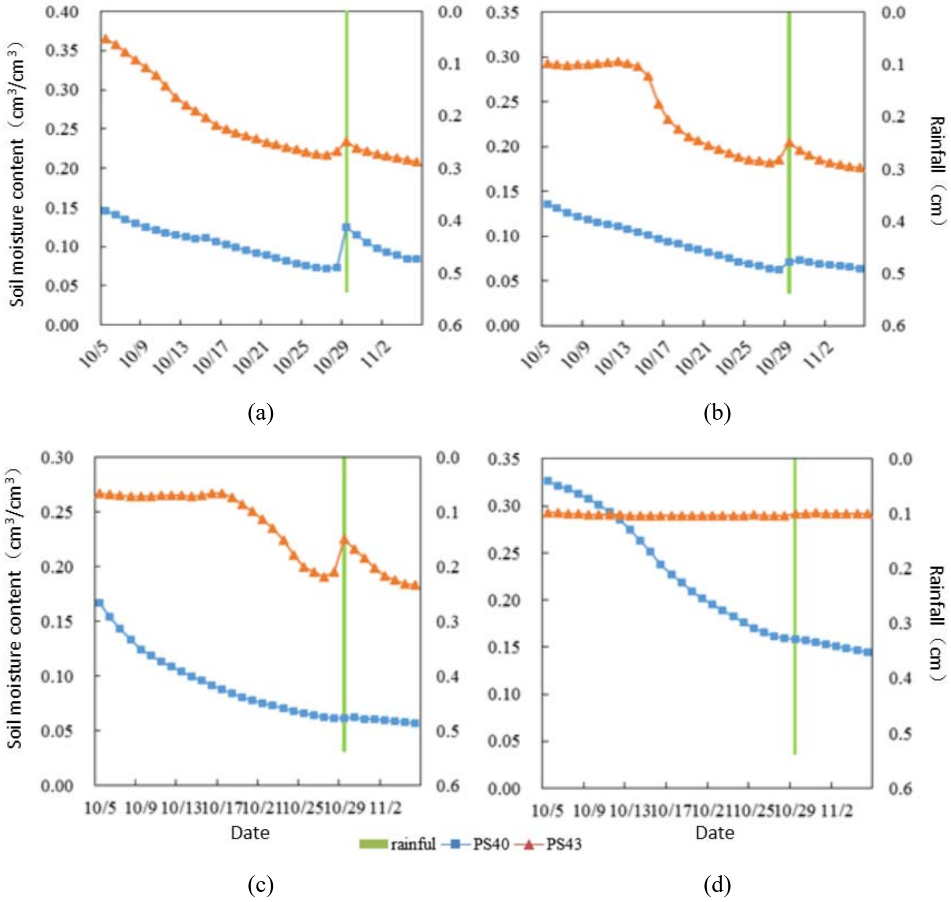

Note: Drought period.

In June 2003 (the humid period, see Figure 8), there was more rainfall and the maximum daily rainfall was 50.28 mm. As shown in Table 6, the *Cv* of the 10–30 cm soil layer under AWF was > 0.3 and thus this soil layer was classified as a fast variable layer. As shown in Figure 8, the curve of soil water content of the 10–30 cm soil layer under AWF showed high variation (without considering the hysteresis effect); the curve rises when the rainfall increases and descended as rainfall decreases. However, there was less change in the curve in the 50 cm soil layer. For UBG, the curve of soil water content showed clear change in amplitude only in the 10 cm soil layer, whereas the curve at 20–50 cm soil layer tends to be stable. The surface soil moisture under the vegetation was most sensitive to rainfall changes. Under the two kinds of vegetation, with the increase in rainfall, the soil moisture content in different soil layers reached the critical value and subsequently the soil moisture content did not increase, but decreased slightly. This was because the soil was saturated, or the rainfall intensity was so large that it produced a high amount of runoff, or the soil water supply by rainfall was less than the soil water consumption and thus rainfall absorption by soil was reduced.

The critical value of the 10 cm soil layer in the AWF was 0.345 cm^3/cm^3 and the soil water content gradually decreased after reaching this value. This may be because the soil was saturated or because of a sudden reduction in rainfall and the soil water supply by rainfall was therefore lower than the soil water consumption. However, the critical value of 10 cm soil under UBG was not easily identified. The critical values of soil water content in the 30 cm and 50 cm soil layers under UBG were 0.2858 and 0.3108 cm^3/cm^3, respectively and soil moisture gradually reduced after reaching these critical values.

Because there was only one rainfall event in October 5 to November 5, 2003 (drought period), the rainfall amount was only 5.39 mm, there was vegetation canopy interception and a litter layer and thus the amount of water absorbed by soil was likely to be small. The soil water content of the two vegetation types showed a decreasing trend due to the lack of supply and until there was rainfall and soil moisture near the surface was increasing (Figure 9). Table 6 indicates that the *Cv* of soil water content in AWF was obviously higher than that in UBG. Figure 9 shows that the decrease rate of soil water content in AWF was higher than that in UBG.

During the humid period, there was a significant positive correlation between the change of soil water content in the 10–30 cm soil layer of AWF and the trend of rainfall and soil moisture increased rapidly during rainfall. However, the relationship between soil moisture content at 50 cm depth and rainfall was relatively weak. Under UBG, the trend of the change of soil moisture at 10 cm depth was consistent with that of rainfall, but there was little change in soil moisture at 20–50 cm depth with rainfall. During the drought period, the *Cv* of soil moisture of AWF was greater than that of UBG in every soil layer. Furthermore, at 50 cm soil depth, the *Cv* of soil water content in AWF was 73 times that in UBG. The soil water content of AWF decreased faster than that of UBG and the latter has a stronger water-holding capacity.

5.4 Explanation of soil moisture response to rainfall

The response of soil moisture to rainfall is a highly complex process, which is affected by rainfall, rainfall intensity, soil physical and chemical properties and vegetation type. Most phenomena of soil moisture change cannot be explained by rainfall infiltration only.

5.4.1 Vegetation root distribution

The roots are one of the main components of the forest ecosystem and the spatial distribution of the roots determines the size of the interaction between the vegetation and the soil environment. The roots of herbaceous vegetation are smaller than those of trees or shrubs and their distribution is relatively shallow, mainly using surface soil water and thus influencing the soil water in surface soil layers.

The AWF in the study area contains two main vegetation types: slash pine and broadleaved tree. The roots of slash pine are well developed and root biomass decreases significantly with the increase of soil depth. The root biomass is largest at 0–20 cm soil depth, accounting for 32.6%–44.7% of total root biomass, whereas the root biomass of 20–40 cm soil accounts for 23.4%–30.4% of the total root biomass. The root biomass of the above two layers account for 63.1%–75.2% of the total root biomass, more than 63% of the root biomass of slash pine centrally distributed in the 0–40 cm soil. In contrast, the root biomass of broad-leaved trees is mainly concentrated at 0–40 cm soil depth, accounting for 74%–99% of the total root biomass and there are few roots in the deeper soil. Bahia grass has a relatively sturdy and lignified root system. About 76.6% of the roots of Bahia grass are distributed in 0–10 cm soil and only 7.8% of roots are distributed below 20 cm soil depth.

Plant roots have a high soil porosity and infiltration rate, which affects rainfall infiltration and the spatial distribution of soil moisture in different layers. When the rainfall conditions are the same, the depth of root distribution and soil moisture changes drastically with rainfall under different vegetation. Therefore, the trend of change in soil moisture in the 10–50 cm soil layer of the AWF in June 2003 humid period was strongly consistent with that of rainfall, whereas in UBG, the soil moisture and rainfall trends were consistent only at 10 cm soil depth.

In the drought period of October 2003, there was little rainfall and the root system was the main channel for vegetation to absorb soil moisture and nutrients. Vegetation growth and transpiration consumed a large quantity of soil moisture and rainfall infiltration of soil moisture supply was less than the consumption of soil moisture, so the soil moisture showed a decreasing trend. Moreover, the evaporation intensity of the AWF was larger than that of the UBG and thus more soil moisture was consumed. Therefore, the soil water content of the AWF was lower than that of the UBG. Surface soil water content (10 cm) of Bahia grassland was relatively low and soil water content increased below 10 cm. This was mainly because the biomass of the ungrazed Bahia grass roots is concentrated in the soil surface and the water consumed by the evaporation of the UBG was mainly from the surface soil water.

5.4.2 Differences in physical and chemical properties of soil under different types of vegetation

The soil infiltration performance and water-holding capacity are directly determined by the soil structure, which is the basis of the dynamic change of soil moisture. Vegetation can also improve the soil structure but there are essential differences between them. The soil in the study area is mainly Myakka fine sand and the litter and organic matter accumulates at the surface of sandy land covered by vegetation. However, the soil organic matter content was lower in the alluvial wetland and the soil is mainly sand at 10–150 cm. In sandy soil, the porosity is low and although the pores are coarse, the number of pores is small.

The root biomass in the AWF is mainly distributed in the soil layer of 0–40 cm, which increases the porosity of the soil, resulting in soil infiltration rate greater than that of the soil layer below 40 cm. Therefore, in the wet period of June 2003, the change of soil moisture in the 10–50 cm soil of the AWF was consistent with the change of rainfall. In contrast, the surface energy of the sand grains was small, the soil water was easily drained and the moisture content was low, thus the soil water content decreased substantially during the drought period.

The contents of organic matter, root biomass and humus were high in the 0–10 cm soil layer of Bahia grassland and the soil bulk density was low. With the increase of depth, soil bulk density increased, coarse grain content increased and the content of organic matter decreased. The soil infiltration rate is large under a low soil bulk density. Therefore, the soil infiltration rate of 10 cm deep soil is larger than that of soil layer below 10 cm, rainfall mainly affects the soil moisture at 10 cm depth in Bahia grassland.

Under different land use patterns, natural grassland has the smallest bulk density and highest soil porosity and thus has a strong water-holding capacity. Moreover, when the rainfall is low, the soil water content of the UBG reduced slowly.

6 Conclusions

Based on the HYDRUS-3D model, the dynamic changes of soil moisture in the wet and dry period of the two kinds of typical vegetation in the study area were analysed using the monitored data and the response to the rainfall was studied. This analysis of the dynamic characteristics of soil moisture under different vegetation types and their relationship with precipitation is helpful to study the interaction between surface water and groundwater and establishing an integrated model of surface water and groundwater.

The main conclusions are as follows:

1. The HYDRUS-3D model had high simulation accuracy for AWF in the study area; however, the simulation of the UBG was less successful. The simulation accuracy of the same vegetation type during the drought period was higher than that of the wet period. The applicability of the HYDRUS-3D model requires further verification.
2. Sensitivity analysis of the soil moisture characteristic curve of the HYDRUS-3D model shows that the saturated water content, θ_s and the pore size index, n, were the most sensitive parameters in the simulation process. The change of the value has a clear effect on the output of the model results and the sensitivity of AWF n was higher than that of UBG.
3. There were significant differences in soil water change characteristics between the two vegetation types. The moisture content at 10–30 cm soil depth decreased with the increase of soil layer and increased at 30–50 cm soil depth. The soil moisture content at 10–30 cm soil depth decreased with the soil increase in the wet period and increased at 30–50 cm soil depth, whereas in the dry period 10–20 cm soil water content decreased, whereas it increased at 20–50 cm soil depth.
4. The mean values of soil moisture of UBG of the wet period at 10–30 cm soil depth and the drought period at 10–50 cm soil depth were higher than those of the AWF. Moreover, the *Cv* of soil water content in each layer of the UBG was lower than that of the AWF in the two periods. The soil water-holding capacity of UBG was stronger than that of the AWF and the UBG was shown to have good water conservation potential.
5. In the wet period, there was a positive correlation between soil moisture content at 10–30 cm soil depth and rainfall in the AWF; however, the consistency at 30–50 cm soil depth was relatively weak. The consistency of changes of soil moisture content at 10 cm soil depth and the rainfall was stronger than that below 10 cm soil depth. The depth of soil impacted by precipitation increased because of the developed root system and smaller soil bulk density of the AWF relative to UBG. Soil water migration to depth was hindered by the shallow root system of the Bahia grass and thus the effect of precipitation on soil moisture of the AWF was higher than that of UBG.

Acknowledgements

This work was supported by the NSFC (No. 41271004) and National Key R&D Program of China (2017YFC0406004).

References

Al-Ogaidi, A.A.M., Wayayok, A., Kamal, M.R. and Abdullah, A.F. (2016) 'Modelling soil wetting patterns under drip irrigation using Hydrus-3D and comparison with empirical models', *Global Conf. Eng. Technol.*

Asim, B., Chauhenry, W., Bedardhaughnangela, K. and Sibing, C. (2017) 'Factors controlling soil water storage in the hummocky landscape of the Prairie Pothole Region of North America', *Can. J. Soil Sci.*, Vol. 92, No. 4, pp.649–663.

Brunetti, G., Simunek, J. and Piro, P. (2016) 'A comprehensive analysis of the variably saturated hydraulic behavior of a green roof in Mediterranean climate', *Vadose Zone J.*, Vol. 5, No. 9, pp.1–17.

Carlisle, V.W., Sodek, F., Collins, M.E., Hammond, L.C. and Harris, W.G. (1985) *Characterization Data for Selected Florida Soils,* University of Florida, IFAS Soil Department, Soil Characterization Laboratory, Gainesville, Florida, USA.

D'Odorico, P., Laio, F., Porporato, A., Ridolfi, L., Rinaldo, A. and Rodrigueziturbe, I. (2010) 'Ecohydrology of terrestrial ecosystems', *Bioscience*, Vol. 60, No. 11, pp.898–907.

Fry, E.L., Pilgrim, E.S., Tallowin, J.R.B., Smith, R.S., Mortimer, S.R. and Beaumont, D.A. (2017) 'Plant, soil and microbial controls on grassland diversity restoration: a long-term, multi-site mesocosm experiment', *J. Appl. Ecol.*, Vol. 3, No. 54, pp.24–47.

Gallego-Elvira, B., Taylor, C.M., Harris, P.P., Ghent, D., Veal, K.L. and Folwell, S.S. (2016) 'Global observational diagnosis of soil moisture control on the land surface energy balance', *Geophys. Res. Lett.*, Vol. 43, No. 6, pp.2623–2631.

Kandelous, M.M. and ŠImůNek, J. (2010) 'Numerical simulations of water movement in a subsurface drip irrigation system under field and laboratory conditions using Hydrus-2D', *Agric. Water Manage.*, Vol. 97, No. 7, pp.1070–1076.

Legates, D.R., Mahmood, R. and Levia, D.F. (2010) 'Soil moisture: a central and unifying theme in physical geography', *Progr. Phys. Geog.*, Vol. 35, No. 1, pp.65–86.

Provenzano, G. (2007) 'Using Hydrus-2D simulation model to evaluate wetted soil volume in subsurface drip irrigation systems', *J. Irrig. Drain. Eng.*, Vol. 133, No. 4, pp.342–349.

Ranatunga, K., Nation, E.R. and Barratt, D.G. (2008) 'Review of soil water models and their applications in Australia', *Environ. Modell. Softw.*, Vol. 23, No. 9, pp.1182–1206.

Sandholt, I., Rasmussen, K. and Andersen, J. (2002) 'A simple interpretation of the surface temperature/vegetation index space for assessment of surface moisture status', *Remote Sens. Environ.*, Vol. 79, No. 2, pp.213–224.

Satchithanantham, S., Krahn, V., Ranjan, R.S. and Sager, S. (2014) 'Shallow groundwater uptake and irrigation water redistribution within the potato root zone', *Agric. Water Manage.*, Vol. 132, No. 3, pp.101–110.

Schlegel, P., Huwe, B. and Teixeira, W.G. (2004) 'Modelling species and spacing effects on root zone water dynamics using Hydrus-2D in an Amazonian agroforestry system', *Agrofor. Syst.*, Vol. 60, No. 3, pp.277–289.

Seneviratne, S.I., Corti, T., Davin, E.L., Hirschi, M., Jaeger, E.B. and Lehner, I. (2010) 'Investigating soil moisture-climate interactions in a changing climate: a review', *Earth Sci. Rev.*, Vol. 99, No. 3, pp.125–161.

Shah, N. (2007) *Vadose Zone Processes Affecting Water Fluctuations: Conceptualization and Modeling Considerations*, University of South Florida, South Florida.

Šimůnek, J., Genuchten, M. and Šejna, M. (2006) *The HYDRUS Software Package for Simulating Two- and Three-dimensional Movement of Water, Heat, and Multiple Solutes in Variably-Saturated Media, Technical Manual*, PC Progress, Prague, Czech Republic.

Šimůnek, J., Genuchten, M.T.V. and Šejna, M. (2008) 'Development and applications of the HYDRUS and STANMOD software packages and related codes', *Vadose Zone J.*, Vol. 72, No. 9, pp.587–600.

Slavich, P.G., Hatton, T.J., Dawes, W.R. and Land, C. (1998) *The Canopy Growth and Transpiration Model of Waves: Technical Description and Evaluation*, Tech. Rep.

Štekauerová, V., Nagy, V. and Kotorová, D. (2006) 'Soil water regime of agricultural field and forest ecosystems', *Biologia*, Vol. 61, No. 19, pp.S300–S304.

Zhang, S.A. and Zhang, Y.Q. (2013) 'Comparative study on application of technical methods for soil moisture monitoring', *J. Chin. Hydrol.*, Vol. 33, pp.25–28.

Zhang, W.G. (2016) *Integrated Development and Application of Soil Water Movement Simulation Software*, Northwest A&F University, Xi'an.